Volume 9 | Number 20 | 21 October 2022

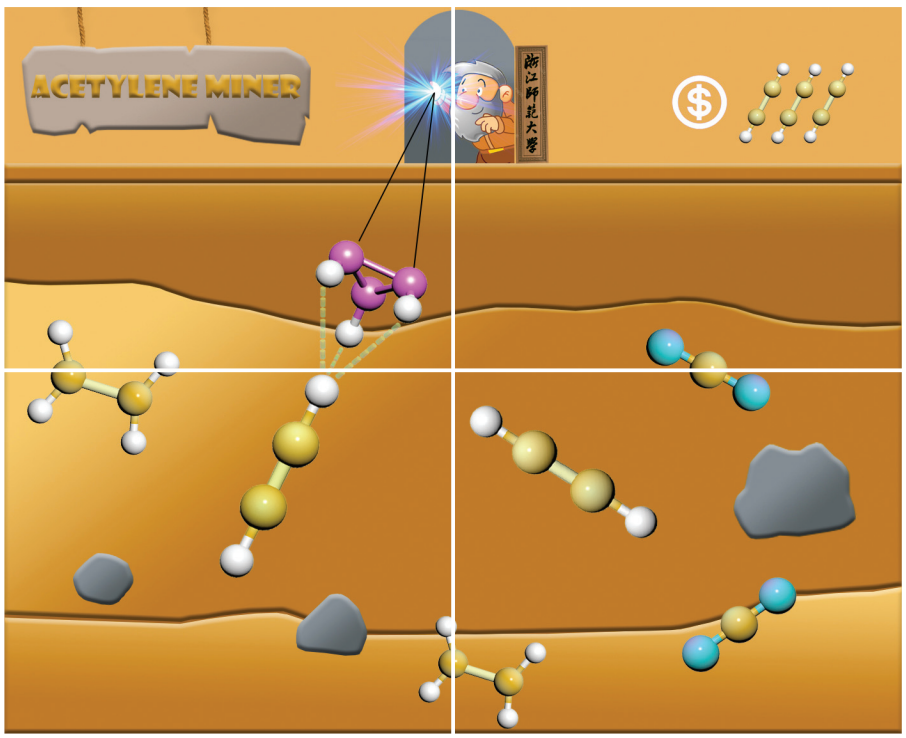


# INORGANIC CHEMISTRY

## FRONTIERS

CCS 中国化学会 CHINESE CHEMICAL SOCIETY
PEKING UNIVERSITY 1898
ROYAL SOCIETY OF CHEMISTRY
rsc.li/frontiers-inorganic

INORGANIC CHEMISTRY FRONTIERS

RESEARCH ARTICLE

View Article Online
View Journal | View Issue



Cite this: *Inorg. Chem. Front.*, 2022, **9**, 5140

# A new boron cluster anion pillared metal organic framework with ligand inclusion and its selective acetylene capture properties†

Wanqi Sun,‡[a] Yujie Jin,‡[b] Yilian Wu,[a] Wushuang Lou,[a] Yanbin Yuan,[a] Simon Duttwyler,[b] Lingyao Wang[a] and Yuanbin Zhang *[a]

Received 25th April 2022,
Accepted 17th July 2022

DOI: 10.1039/d2qi00890d

rsc.li/frontiers-inorganic

The separation of acetylene ($C_2H_2$) from carbon dioxide ($CO_2$) and ethylene ($C_2H_4$) is important in industry but challenging due to their similar physical properties. Herein, a novel microporous boron cluster pillared metal–organic framework BSF-10 was synthesized with ligand inclusion for efficient $C_2H_2/CO_2$ and $C_2H_2/C_2H_4$ adsorption separation. The free dipyridyl ligands in the large pore reduce the porosity of BSF-10 but stabilize the framework. The available narrow pores without inclusion of ligands are suited for the accommodation of $C_2H_2$ by cooperative dihydrogen bonding. High $C_2H_2$ capacity and high $C_2H_2$ selectivity over $CO_2$ and $C_2H_4$ are achieved. The practical separation ability was confirmed by the breakthroughs using $C_2H_2/CO_2$ and $C_2H_2/C_2H_4$ gas mixtures with good recyclability. The dynamic separation factor of 2.8 for the equimolar $C_2H_2/CO_2$ mixture is comparable to those of many benchmark materials.



The separation of $C_2H_2/CO_2$ and $C_2H_2/C_2H_4$ to produce $C_2H_2$ and $C_2H_4$ in high purity is important in industry.[1–4] $C_2H_2$ is a vital fundamental material for the synthesis of various organic chemicals and polymers. Produced from the cracking of hydrocarbons or partial combustion of natural gas, $CO_2$ is a contaminant and needs to be removed.[3] On the other hand, the deep removal of $C_2H_2$ is a must in the process of ethylene production to obtain polymer grade $C_2H_4$ (>99.996%) since trace $C_2H_2$ can poison the ethylene polymerization catalysts by forming metal acetylides.[4] Current state-of-the-art technologies for the separation and purification of $C_2H_2$ from other gases largely rely on cryogenic distillation, partial hydrogenation, or solvent extraction, which are either energy-intensive or associated with pollution. When compared, physisorption separation using porous materials is more energy-efficient and eco-friendly.[1,2] However, due to their similar molecular diameter and polarity (Table S1†), efficient $C_2H_2/CO_2$ and $C_2H_2/C_2H_4$ separation is still difficult to achieve.

The design of advanced porous materials is vital for many applications such as gas separation[5] and catalysis.[6] Recent years have witnessed families of porous metal organic frameworks (MOFs) with excellent properties for physisorption separations.[7–16] In this context, inorganic anion pillared MOFs as a unique subclass with strong Lewis basic functional anion sites, developed firstly by the Zaworotko group[17] and Kitagawa group,[18] have been of particular interest for selective gas separation due to their high molecular recognition competence. These inorganic anion pillared MOFs can be classified to five series to date according to the anions used: (1) MFSIX networks pillared by hexafluorometallate anions (*e.g.* $SiF_6^{2-}$, $GeF_6^{2-}$, and $TiF_6^{2-}$),[19,20] (2) $MO_xF_y$ pillared networks with anions containing octahedral metal centers bonded through both O and F atoms (*e.g.* $NbOF_5^{2-}$ and $TaOF_5^{2-}$),[21–23] (3) networks cross-linked by tetrahedral $MO_4^{2-}$ oxyanions (*e.g.* $CrO_4^{2-}$, $MoO_4^{2-}$, $SO_4^{2-}$),[24] (4) DICRO coordination networks that are sustained with $Cr_2O_7^{2-}$ dianions,[25] and (5) boron cluster anion pillared supramolecular metal organic frameworks (BSFs) featuring *closo*-$[B_{12}H_{12}]^{2-}$ or *closo*-$[B_{12}H_{11}I]^{2-}$ as the inorganic pillars.[26–32]

The icosahedral *closo*-dodecaborate $[B_{12}H_{12}]^{2-}$ is a stable dianionic boron cluster consisting of 12 identical B–H vertices (Fig. 1A).[33] It is considered as a three-dimensional aromatic analogue to two-dimensional aromatic benzene due to the electron delocalization.[34] While other anions use electronegative F and O to coordinate transition metals, $[B_{12}H_{12}]^{2-}$ utilizes hydride, which is not common in coordination polymers. In 2019, we reported the first BSF material termed BSF-1, which

[a]*Key Laboratory of the Ministry of Education for Advanced Catalysis Materials, College of Chemistry and Life Sciences, Zhejiang Normal University, Jinhua 321004, China. E-mail: ybzhang@zjnu.edu.cn*
[b]*Department of Chemistry, Zhejiang University, 38 Zheda Road, 310027 Hangzhou, P. R. China*

†Electronic supplementary information (ESI) available. CCDC 2168393 and 2168394. For ESI and crystallographic data in CIF or other electronic format see DOI: https://doi.org/10.1039/d2qi00890d

‡These authors contributed equally to this work.

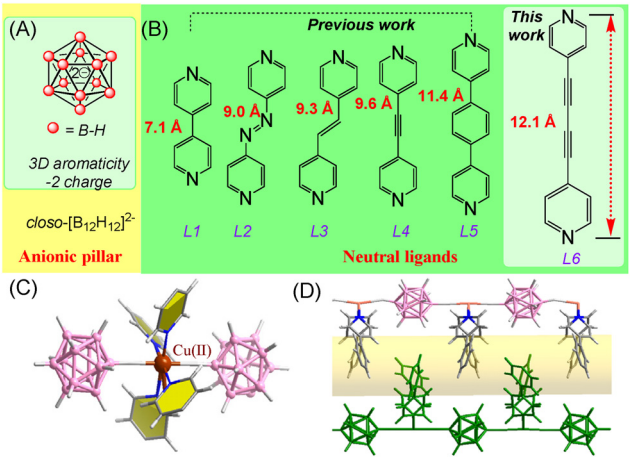


**Fig. 1** (A and B) Structure of *closo*-dodecaborate $[B_{12}H_{12}]^{2-}$ and organic ligands. (C) General coordination mode in BSFs. (D) General 1D pore channels of interpenetrated BSFs.

is constructed from *closo*-$[B_{12}H_{12}]^{2-}$ dianions, $Cu^{2+}$ ions and 1,2-di(pyridin-4-yl)ethyne (L4, Fig. 1B) with N···Cu and B–H···Cu coordination as well as B–H···H–C dihydrogen bonds (Fig. 1C).[26] Every hexacoordinate Cu center serves as a six-connected node. Four pyridyl units from different ligands comprise the equatorial plane and the axial positions of the Cu nodes coordinate to hydrogen atoms from $[B_{12}H_{12}]^{2-}$, which bridge two Cu nodes to generate an infinite Cu-dodecaborate chain (Fig. 1D). BSF-1 displays high separation selectivity for $C_3H_8/CH_4$ and $C_2H_6/CH_4$. The extension of the organic linker to L5 (Fig. 1B) produces a isostructural MOF BSF-3 with improved porosity, which shows superior $C_2H_2$ capacity as well as enhanced $C_2H_2/C_2H_4$ and $C_2H_2/CO_2$ separation selectivity compared to BSF-1.[28] BSF-4 with L2 and BSF-9 with L3 were expected to show similar gas separation performance due to the similar length of organic linkers.[29,30] However, the interpenetration symmetry difference endows BSF-9 with symmetrical interpenetration mode and a record high $C_2H_2/CO_2$ separation selectivity in robust MOFs without open metal sites, which is over 5 fold that in BSF-4 with asymmetrical interpenetration mode.[30] Another approach to tune the porosity of BSFs is to alter the interpenetration degree. Eliminating the interpenetration of BSFs by controlling the binary solvent system can afford enhanced theoretical porosity. However, these non-interpenetrated MOFs (*eg*, BSF-5, 6, 7, 8) are actually very unstable and lose most of the porosity after guest removal due to the framework collapse.[30] Thus, it is still very challenging to design BSFs with a desirable stable porous structure and the interpenetration mode in BSFs is still difficult to predict and control.

Herein, we would like to report another approach to tune the porosity and stability of BSFs. 1,4-di(pyridin-4-yl)buta-1,3-diyne (L6, Fig. 1B) with a N···N distance of 12.1 Å and negligible steric hindrance was utilized as the organic linker. A new boron cluster anion pillared metal organic framework BSF-10 with ligand inclusion was prepared. BSF-10 is asymmetrically interpenetrated. There is one large pore with a square shaped window and two small pores with narrow rectangular shaped windows. In the large pore, L6 is included and unable to be removed by soaking into polar solvents or heating under vacuum. This ligand inclusion reduces the porosity of BSF-10 but enhances the stability for practical applications, which has never been reported in BSFs.[6] The available narrow pores without inclusion of ligands are suited for the accommodation of $C_2H_2$ by cooperative dihydrogen bonding. Thus, the high capacity of $C_2H_2$ (65.0 $cm^3$ $g^{-1}$) as well as good separation selectivity for $C_2H_2/CO_2$ (13.52–5.86) and $C_2H_2/C_2H_4$ (4.09–2.93) under ambient conditions are achieved. The practical separation ability was further confirmed by the dynamic breakthroughs using $C_2H_2/CO_2$ and $C_2H_2/C_2H_4$ gas mixtures with good recyclability. The dynamic separation factor of 2.8 for equimolar $C_2H_2/CO_2$ mixtures is comparable to those of many benchmark materials.

BSF-10 was readily prepared by stirring a mixture of $Na_2[B_{12}H_{12}]\cdot 2H_2O$, $Cu(NO_3)_2\cdot 3H_2O$ and L6 in MeOH at 35 °C for 48 h. Single crystals of BSF-10 were produced by layering a MeOH solution of L6 onto an aqueous solution of $Na_2[B_{12}H_{12}]\cdot 2H_2O$ and $Cu(NO_3)_2\cdot 3H_2O$. X-ray structural analysis of BSF-10 revealed that it crystallizes in a three-dimensional (3D) framework in the monoclinic space group *P*21/*c* (Table S2†). The asymmetric interpenetration leads to the generation of two kinds of pore channels: large Pore I and small Pores II/III (Fig. 2A). The large Pore I features a square shaped window and the small Pores II/III display narrow rec-

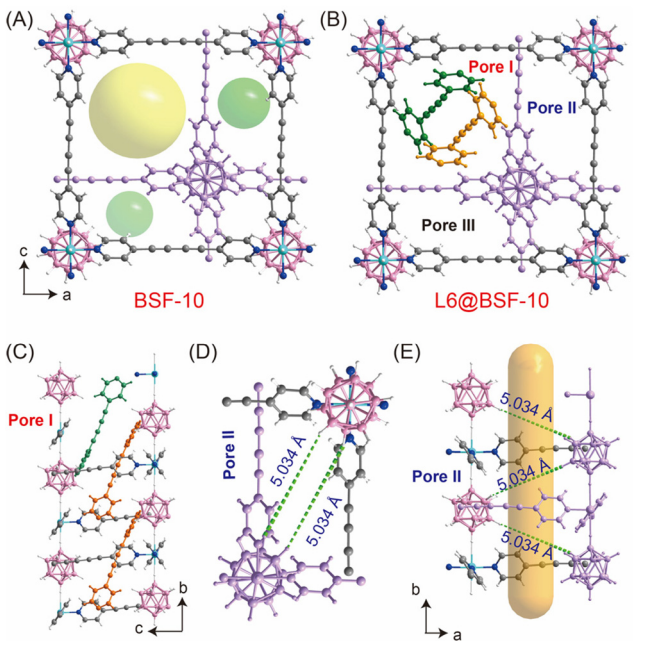


**Fig. 2** Porous structure of BSF-10. (A) Generation of two kinds of pores by asymmetrical interpenetration. (B) L6 included in the large Pore I. (C) The packing mode of L6 in Pore I. (D and E) Structure of Pore II in two directions highlighting the closest B–H···H–B distance after subtracting the two van der Waals radii of hydrogen.

tangular shaped windows. Notably, L6 is included in the large pore, and unable to be removed by soaking BSF-10 into polar solvents or heating under vacuum (Fig. 2B). Analysis of the configuration of L6 indicates the existence of two forms of L6 in Pore I with a packing mode of AABB (Fig. 2C). Strong π···π interactions among guests as well as multiple weak B–H···H–C interaction exist, which stabilize the structure of L6@BSF-10 and prevent the release of L6. Notably, the $Cu[B_{12}H_{12}]$ : L6 ratio has no influence on the structure of BSF-10. Even when excess $Cu[B_{12}H_{12}]$ was used, the single crystals still show the composition of $Cu[B_{12}H_{12}](L6)_3$ with free L6 inside Pore I (Table S3†).

Pore II and Pore III are nearly identical. The closest distance between two opposite B–H units in BSF-10 is 5.034 Å (Fig. 2D and E). This distance is suited to trap an acetylene molecule by cooperative dihydrogen bonding ($B–H^{\delta-}\cdots H^{\delta+}$-CC-$H^{\delta+}\cdots H^{\delta-}$–B)[28] and thus be potential for $C_2H_2/CO_2$ and $C_2H_2/C_2H_4$ separation. Besides, the pore window size of *ca.* 4 Å (Fig. 3) defined by the opposite H(Py)···H(Py) is also close to the diameter of $C_2H_2$ (kinetic diameter 3.3 Å, 3D diameter: 3.32 × 3.34 × 5.70 $Å^3$), allowing tight $C_2H_2$ accommodation.

Inspired by the structural analysis, we were interested to investigate the potential of BSF-10 for the selective adsorption separation of $C_2H_2$ from $CO_2$ and $C_2H_4$. The first step is to confirm the permanent porosity of BSF-10 after solvent removal as BSFs with larger pores are not stable upon activation.[31] $N_2$ gas adsorption experiments at 77 K were conducted after activating BSF-10 under vacuum at 75 °C for 12 h. A typical Type I isotherm was observed, indicating the microporous character of BSF-10. The BET surface area was calculated to be 426.3 $m^2\ g^{-1}$ with a total pore volume of 0.216 $cm^3\ g^{-1}$ at $P/P_0$ = 0.95, (Fig. 4A), which is quite close to the calculated pore volume of 0.222 $cm^3\ g^{-1}$ based on the single crystal structure of BSF-10 using a probe with the radius of 1.2 Å (Fig. 3).

The establishment of permanent microporosity in BSF-10 motivated us to study the gas separation performance for $C_2H_2/CO_2$ and $C_2H_2/C_2H_4$. First of all, single component adsorption isotherms of $C_2H_2$, $CO_2$ and $C_2H_4$ were collected under 298 and 278 K. At 1.0 bar, the $C_2H_2/CO_2/C_2H_4$ uptakes were 65.0/25.8/39.5 $cm^3\ g^{-1}$ at 298 K and 78.1/53.0/40.2 $cm^3\ g^{-1}$ at 278 K, respectively (Fig. 4B and C). The isosteric heat of adsorption ($Q_{st}$) for BSF-10 was then calculated using the Clausius–Clapeyron equation after fitting the isotherms to the Langmuir–Freundlich equation with excellent accuracy ($R^2$ > 0.9999, Tables S4 and 5†). $Q_{st}$ values at near-zero loading for $C_2H_2$, $CO_2$, and $C_2H_4$ were 34.8, 27.4, and 22.9 kJ $mol^{-1}$ (Fig. 4D). This trend of $Q_{st}$ values is consistent with the slope of the adsorption isotherms, indicating the preferential adsorption of $C_2H_2$ over $CO_2$ and $C_2H_4$.

Additionally, the $Q_{st}$ value for $C_2H_2$ in BSF-10 is higher than that of BSF-1 (30.7 kJ $mol^{-1}$), but lower than that of BSF-3 (42.7 kJ $mol^{-1}$), consistent with the $C_2H_2$ adsorption uptake trend of BSF-1 (2.35 mmol $g^{-1}$) < BSF-10 (2.90 mmol $g^{-1}$) < BSF-3 (3.59 mmol $g^{-1}$). Notably, this modest $Q_{st}$ renders BSF-10 a suitable porous material for practical application with a low energy footprint for regeneration.

Since selectivity is as important as capacity to evaluate the separation performance, the $C_2H_2/CO_2$ and $C_2H_2/C_2H_4$ selectivity on BSF-10 at 298 K and 278 K was calculated using ideal adsorbed solution theory (IAST), which revealed that the selectivity for equimolar $C_2H_2/CO_2$ and $C_2H_2/C_2H_4$ at 298 K and 1.0 bar was 13.52–5.86 and 4.09–2.93, respectively (Fig. 5A). The selectivity is slightly increased under low pressure when the temperature reduced to 278 K, and is 17.4–5.2 for $C_2H_2/CO_2$ and 4.8–2.8 for $C_2H_2/C_2H_4$ (Fig. 5B). The $C_2H_2/CO_2$ selectivity with different $C_2H_2$ molar ratios was further calculated for BSF-10, which indicates that the decrease of the $C_2H_2$ molar ratio leads to the increased $C_2H_2/CO_2$ selectivity (Fig. 5C). The $C_2H_2$ capacity and the $C_2H_2/CO_2$ selectivity on BSF-10 are superior to those of many well-performing materials such as BSF-1 (52.5 $cm^3\ g^{-1}$, $S$ = 3.4),[26]

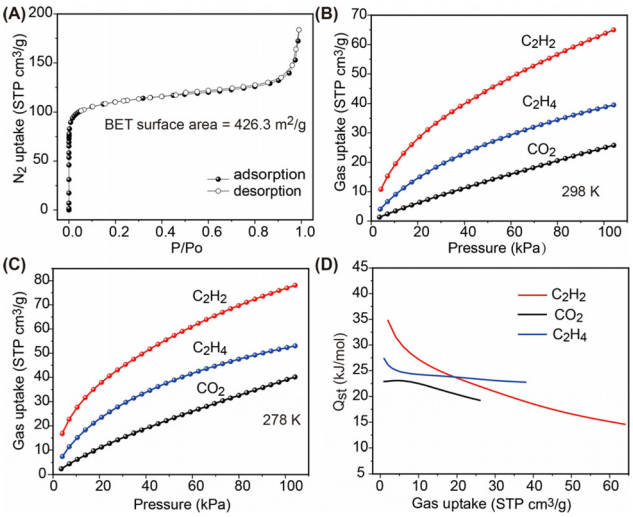


**Fig. 4** (A) $N_2$ adsorption and desorption isotherms of BSF-10. (B and C) Single component adsorption isotherms of $C_2H_2$, $CO_2$ and $C_2H_4$ on BSF-10 at 298 and 278 K. (D) Adsorption heats of $C_2H_2$, $CO_2$ and $C_2H_4$ on BSF-10.

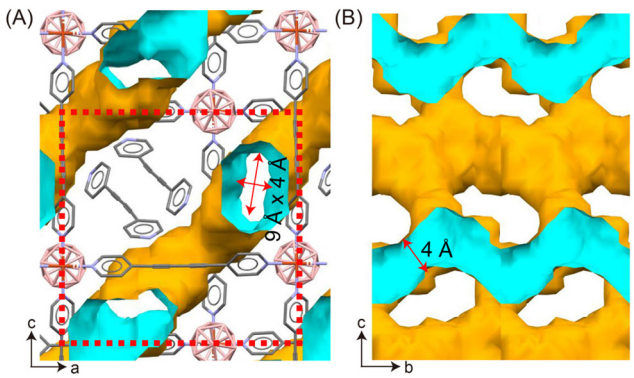


**Fig. 3** Voids and pore windows of BSF-10 generated by a probe with the radius of 1.2 Å seen along (A) *b*-axis and (B) *a*-axis. The pore window dimensions are determined after subtracting the two van der Waals radii of hydrogen.

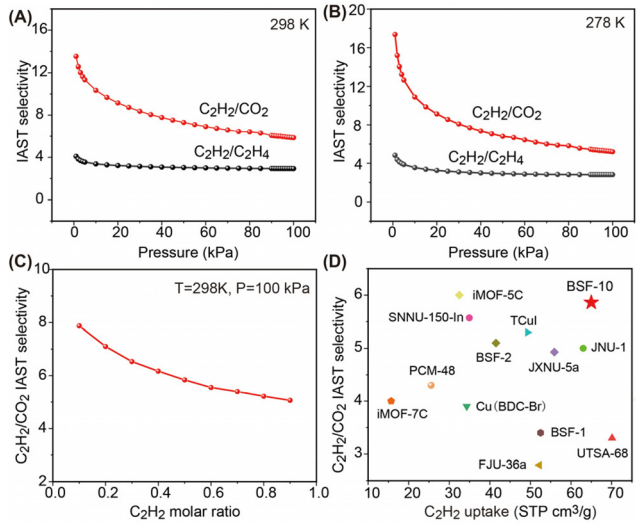


Fig. 5 (A and B) IAST selectivity of $C_2H_2/CO_2$ and $C_2H_2/C_2H_4$ at 298 and 278 K. (C) IAST selectivity of $C_2H_2/CO_2$ with different $C_2H_2$ molar ratios. (D) Comparison of the $C_2H_2$ uptakes and $C_2H_2/CO_2$ selectivity among BSF-10 and others well-performing MOFs.

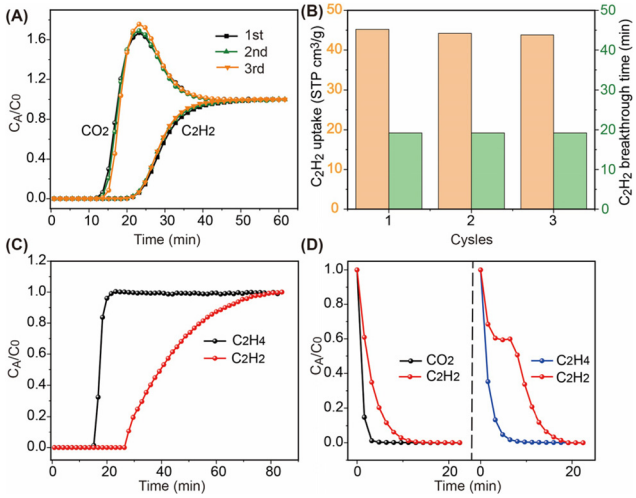


Fig. 7 (A) Experimental breakthrough curves of $C_2H_2/CO_2$ (50/50) on BSF-10 at 298 K. (B) Comparison of the dynamic $C_2H_2$ uptake from the $C_2H_2/CO_2$ (50/50) mixture and breakthrough time among three cycles of breakthrough experiments. (C) Experimental breakthrough curves of $C_2H_2/C_2H_4$ (1/99) on BSF-10 at 298 K. (D) The desorption curves of BSF-10 after breakthrough experiments of $C_2H_2/CO_2$ (50/50) mixtures and $C_2H_2/C_2H_4$ (1/99) mixtures.

BSF-2 (41.5 $cm^3\ g^{-1}$, $S$ = 5.1),[27] TCuI (49.3 $cm^3\ g^{-1}$, $S$ = 5.3),[35] JNU-1 (63 $cm^3\ g^{-1}$, $S$ = 5),[36] iMOF-7C (15.7 $cm^3\ g^{-1}$, $S$ = 4),[37] FJU-36a (52.2 $cm^3\ g^{-1}$, $S$ = 2.8),[38] SNNU-150-In (34.9 $cm^3\ g^{-1}$, $S$ = 5.6),[39] PCM-48 (25.5 $cm^3\ g^{-1}$, $S$ = 4.3),[40] and JXNU-5a (55.9 $cm^3\ g^{-1}$, $S$ = 5),[41] (Fig. 5D), but inferior to those of BSF-3 (80.4 $cm^3\ g^{-1}$, $S$ = 16.3).[28] The $C_2H_2/CO_2$ uptake ratio of 2.52 at 298 K and 1 bar is also relatively high. This value is superior to those of most MOFs that separate $C_2H_2/CO_2$ by a thermodynamic mechanism,[42–52] but slightly lower than those of $Cu^I$@UiO66-$(COOH)_2$ (2.58),[43] MAF-2 (3.68),[47] and SIFSIX-21-Ni (3.1)[17c] as shown in Fig. 6 and Table S8.†

To confirm the practical separation ability of BSF-10 for $C_2H_2/CO_2$ and $C_2H_2/C_2H_4$ mixtures, dynamic breakthrough experiments were conducted. 0.233 g of BSF-10 powder was packed into a stainless column with a size of Φ 4.6 mm × 5 cm. After activating the sample by Ar purge at 75 °C for 12 h, an equimolar $C_2H_2/CO_2$ mixture was introduced. $CO_2$ appeared at the outlet within 12 min while $C_2H_2$ was retained in the column until 20 min (Fig. 7A). After complete breakthrough, Ar gas with a flow rate of 5 mL $min^{-1}$ was used to desorb the adsorbed $C_2H_2$ and $CO_2$ gases as well as to regenerate the material. Notably, nearly all the $C_2H_2$ and $CO_2$ gases are desorbed within 20 min at 75 °C and the material is regenerated for further use (Fig. 7D). Calculation of the areas of the breakthrough curves and desorption curves indicated that BSF-10 has a dynamic $C_2H_2$ capacity of 45 $cm^3\ g^{-1}$ with a $C_2H_2/CO_2$ separation factor of 2.8. This separation factor is slightly lower than that of benchmark materials such as CAU-10-H (3.4),[42] $Cu^I$@UiO-66-$(COOH)_2$ (3.4)[43] and JCM-1 (4.4),[44] but higher than that of NKMOF-1-Ni (2.6),[45] FJU-90 (2.1)[46] and HOF-3a (2).[53] Besides, the dynamic $C_2H_2$ capacity of BSF-10 is also comparable to that of JCM-1 (49.3 $cm^3\ g^{-1}$). The regenerated BSF-10 was further used for repeated tests. Nearly no performance reduction was observed over 3 cycles (Fig. 7B). The same sample was further used for $C_2H_2/C_2H_4$ (1/99) mixture breakthrough experiments. $C_2H_4$ was detected at 15 min and $C_2H_2$ at 28 min, suggesting a good capture ability of trace $C_2H_2$ from bulky $C_2H_4$ (Fig. 7C). Desorption curves further indicated that the captured $C_2H_2$ can be desorbed within 20 min by Ar purge at 75 °C (Fig. 7D). Combining the high dynamic $C_2H_2$ capacity, high separation factor as well as facile regeneration conditions, BSF-10 is a good candidate for practical $C_2H_2/CO_2$ and $C_2H_2/C_2H_4$ separation.

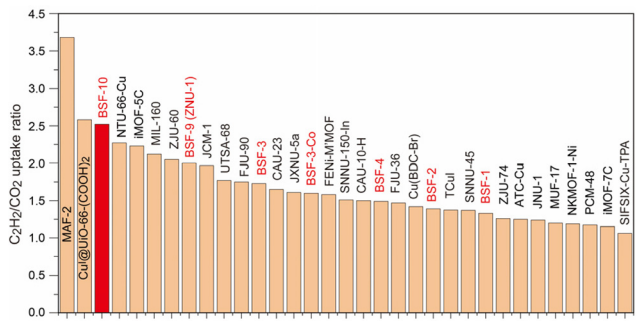


Fig. 6 Comparison of the $C_2H_2/CO_2$ uptake ratios at 298 K and 1 bar among BSF-10 and other well-performing materials in the context of $C_2H_2/CO_2$ separation by a thermodynamic mechanism.

In conclusion, we prepared a novel microporous boron cage pillared metal–organic framework BSF-10 with unprecedented ligand inclusion. Free dipyridyl ligands occupy the large pores and interact with the framework by multiple interactions, which reduces the porosity of BSF-10 but enhances the stability of the framework. The narrow pores without inclusion of

ligands are suited for the selective accommodation of $C_2H_2$ by cooperative dihydrogen bonding. Thus, high $C_2H_2$ capacity and high $C_2H_2$ selectivity over $CO_2$ and $C_2H_4$ are achieved. The practical separation ability was completely confirmed by the breakthroughs using $C_2H_2/CO_2$ and $C_2H_2/C_2H_4$ gas mixtures with good recyclability and facile regeneration conditions. The dynamic separation factor of 2.8 for the equimolar $C_2H_2/CO_2$ mixture is comparable to those of many benchmark materials. Boron cage pillared metal–organic frameworks constructed by non-linear organic linkers are under exploration. Besides, MOFs with dual $C_2H_2/C_2H_4$ and $C_2H_2/CO_2$ separation ability will be increasingly important for separating multicomponent gas mixtures using a single adsorbent, which currently largely relies on synergistic/tandem packed adsorbents in fixed-beds.[54]

## Conflicts of interest

There are no conflicts to declare.

## Acknowledgements

Y. Zhang thanks the support of the Natural Science Foundation of China (No. 21908193) and Jinhua Industrial Key Project (2021A22648). L. Wang thanks the support of Open Research Fund of Key Laboratory of the Ministry of Education for Advanced Catalysis Materials and Zhejiang Key Laboratory for Reactive Chemistry on Solid Surfaces, Zhejiang Normal University (KLMEACM202111). S. Duttwyler thanks the support of the National Natural Science Foundation of China (No. 21871231) and the Special Funds for Basic Scientific Research of Zhejiang University (No. 2019QNA3010 and K20210335).



## Notes and references

1 D. S. Sholl and R. P. Lively, Seven chemical separations to change the world, *Nature*, 2016, **532**, 435–438.

2 K. Adil, Y. Belmabkhout, R. S. Pillai, A. Cadiau, P. M. Bhatt, A. H. Assen, G. Maurin and M. Eddaoudi, Gas/vapour separation using ultra-microporous metal-organic frameworks: insights into the structure/separation relationship, *Chem. Soc. Rev.*, 2017, **46**, 3402–3430.

3 W. Sun, J. Hu, Y. Jiang, N. Xu, L. Wang, J. Li, Y. Hu, S. Duttwyler and Y. Zhang, Flexible molecular sieving of $C_2H_2$ from $CO_2$ by a new cost-effective metal organic framework with intrinsic hydrogen bonds, *Chem. Eng. J.*, 2022, **439**, 135745.

4 X. Cui, K. Chen, H. Xing, Q. Yang, R. Krishna, Z. Bao, H. Wu, W. Zhou, X. Dong, Y. Han, B. Li, Q. Ren, M. J. Zaworotko and B. Chen, Pore chemistry and size control in hybrid porous materials for acetylene capture from ethylene, *Science*, 2016, **353**, 141–144.

5 (*a*) H. Zeng, M. Xie, T. Wang, R.-J. Wei, X.-J. Xie, Y. Zhao, W. Li and D. Li, Orthogonal-array dynamic molecular sieving of propylene/propane mixtures, *Nature*, 2021, **595**, 542–548; (*b*) Y. Chai, X. Han, W. Li, S. Liu, S. Yao, C. Wang, W. Shi, I. Da-Silva, P. Manuel, Y. Cheng, L. D. Daemen, A. J. Ramirez-Cuesta, C. C. Tang, L. Jiang, S. Yang, N. Guan and L. Li, Control of zeolite pore interior for chemo-selective alkyne/olefin separations, *Science*, 2020, **368**, 1002–1006; (*c*) N. Kumar, S. Mukherjee, A. Bezrukov, M. Vandichel, M. Shivanna, D. Sensharma, A. Bajpai, V. Gascon, K. Otake, S. Kitagawa and M. J. Zaworotko, A square lattice topology coordination network that exhibits highly selective $C_2H_2/CO_2$ separation performance, *SmartMat*, 2020, **1**, e1008; (*d*) S. Sharma, S. Mukherjee, A. V. Desai, M. Vandichel, G. K. Dam, A. Jadhav, G. Kociok-Kohn, M. J. Zaworotko and S. K. Ghosh, Efficient Capture of Trace Acetylene by an Ultramicroporous Metal-Organic Framework with Purine Binding Sites, *Chem. Mater.*, 2021, **33**, 5800–5808; (*e*) Z. Yao, Z. Zhang, L. Liu, Z. Liu, W. Zhou, Y. Zhao, Y. Han, B. Chen, R. Krishna and S. Xiang, Extraordinary Separation of Acetylene-Containing Mixtures with Microporous Metal-Organic Frameworks with Open O Donor Sites and Tunable Robustness through Control of the Helical Chain Secondary Building Units, *Chem. – Eur. J.*, 2016, **22**, 5676–5683; (*f*) L. Feng, G. S. Day, K. Y. Wang, S. Yuan and H. C. Zhou, Strategies for Pore Engineering in Zirconium Metal-Organic Frameworks, *Chem*, 2020, **6**, 2902–2923; (*g*) Z. Ji, H. Wang, S. Canossa, S. Wuttke and O. M. Yaghi, Pore Chemistry of Metal-Organic Frameworks, *Adv. Funct. Mater.*, 2020, **30**, 2000238.

6 (*a*) S. Naghdi, A. Cherevan, A. Giesriegl, R. Guillet-Nicolas, S. Biswas, T. Gupta, J. Wang, T. Haunold, B. C. Bayer, G. Rupprechter, M. C. Toroker, F. Kleitz and D. Eder, Selective ligand removal to improve accessibility of active sites in hierarchical MOFs for heterogeneous photocatalysis, *Nat. Commun.*, 2022, **13**, 282; (*b*) T. Qian, C. Zhao, R. Wang, X. Chen, J. Hou, H. Wang and H. Zhang, Synthetic azobenzene-containing metal-organic framework ion channels toward efficient light-gated ion transport at the subnanoscale, *Nanoscale*, 2021, **13**, 17396–17403.

7 P.-Q. Liao, N.-Y. Huang, W.-X. Zhang, J.-P. Zhang and X.-M. Chen, Controlling guest conformation for efficient purification of butadiene, *Science*, 2017, **356**, 1193–1196.

8 X. Zhao, Y. Wang, D. S. Li, X. Bu and P. Feng, Metal-Organic Frameworks for Separation, *Adv. Mater.*, 2018, **30**, 1705189.

9 J.-W. Zhang, W.-J. Ji, M.-C. Hu, S.-N. Li, Y.-C. Jiang, X.-M. Zhang, P. Xu and Q.-G. Zhai, A superstable 3p-block metal-organic framework platform towards prominent $CO_2$ and $C_1/C_2$-hydrocarbon uptake and separation performance and strong Lewis acid catalysis for $CO_2$ fixation, *Inorg. Chem. Front.*, 2019, **6**, 813–819.

10 R.-B. Lin, L. Li, H.-L. Zhou, H. Wu, C. He, S. Li, R. Krishna, J. Li, W. Zhou and B. Chen, Molecular sieving of ethylene from ethane using a rigid metal-organic framework, *Nat. Mater.*, 2018, **17**, 1128–1133.

11 P.-D. Zhang, X.-Q. Wu, T. He, L.-H. Xie, Q. Chen and J.-R. Li, Selective adsorption and separation of $C_2$ hydro-

 

carbons in a "flexible-robust" metal-organic framework based on a guest-dependent gate-opening effect, *Chem. Commun.*, 2020, **56**, 5520–5523.

12 M. K. Taylor, T. Runčevski, J. Oktawiec, J. E. Bachman, R. L. Siegelman, H. Jiang, J. A. Mason, J. D. Tarver and J. R. Long, Near-Perfect $CO_2/CH_4$ Selectivity Achieved through Reversible Guest Templating in the Flexible Metal-Organic Framework Co(bdp), *J. Am. Chem. Soc.*, 2018, **140**, 10324–10331.

13 Y. Zhang, X. Cui and H. Xing, Recent advances in the capture and abatement of toxic gases and vapors by metal-organic frameworks, *Mater. Chem. Front.*, 2021, **5**, 5970–6013.

14 D. Lv, P. Zhou, J. Xu, S. Tu, F. Xu, J. Yan, H. Xi, W. Yuan, Q. Fu, X. Chen and Q. Xia, Recent advances in adsorptive separation of ethane and ethylene by $C_2H_6$-selective MOFs and other adsorbents, *Chem. Eng. J.*, 2022, **431**, 133208.

15 P. Liu, K. Chen, Y. Chen, X. Wang, J. Yang, L. Li and J. Li, Linker micro-regulation of a Hofmann-based metal-organic framework for efficient propylene/propane separation, *Inorg. Chem. Front.*, 2022, **9**, 1082–1090.

16 H. Li, K. Wang, Y. Sun, C. T. Lollar, J. Li and H.-C. Zhou, Recent advances in gas storage and separation using metal-organic frameworks, *Mater. Today*, 2018, **21**, 108–121.

17 (*a*) S. Subramanian and M. J. Zaworotko, Porous Solids by Design: $[Zn(4,4'\text{-bpy})_2(SiF_6)]_n \cdot xDMF$, a Single Framework Octahedral Coordination Polymer with Large Square Channels, *Angew. Chem., Int. Ed. Engl.*, 1995, **34**, 2127–2129; (*b*) S. Mukherjee, N. Kumar, A. A. Bezrukov, K. Tan, T. Pham, K. A. Forrest, K. A. Oyekan, O. T. Qazvini, D. G. Madden, B. Space and M. J. Zaworotko, Amino-Functionalised Hybrid Ultramicroporous Materials that Enable Single-Step Ethylene Purification from a Ternary Mixture, *Angew. Chem., Int. Ed.*, 2021, **60**, 10902–10909; (*c*) N. Kumar, S. Mukherjee, N. C. Harvey-Reid, A. A. Bezrukov, K. Tan, V. Martins, M. Vandichel, T. Pham, P. E. Kruger and M. J. Zaworotko, Breaking the trade-off between selectivity and adsorption capacity for gas separation, *Chem*, 2021, **7**, 3085–3098.

18 S. Noro, S. Kitagawa, M. Kondo and K. Seki, A New, Methane Adsorbent, Porous Coordination Polymer [{CuSiF6(4,4′-bipyridine)2}n], *Angew. Chem., Int. Ed.*, 2000, **39**, 2081–2084.

19 Y. Jiang, J. Hu, L. Wang, W. Sun, N. Xu, R. Krishna, S. Duttwyler, X. Cui, H. Xing and Y. Zhang, Comprehensive Pore Tuning in an Ultrastable Fluorinated Anion Cross-Linked Cage-Like MOF for Simultaneous Benchmark Propyne Recovery and Propylene Purification, *Angew. Chem., Int. Ed.*, 2022, **61**, e20220094.

20 Q. Dong, X. Zhang, S. Liu, R.-B. Lin, Y. Guo, Y. Ma, A. Yonezu, R. Krishna, G. Liu, J. Duan, R. Matsuda, W. Jin and B. Chen, Tuning Gate-Opening of a Flexible Metal-Organic Framework for Ternary Gas Sieving Separation, *Angew. Chem., Int. Ed.*, 2020, **59**, 22756–22762.

21 X. Cui, Z. Niu, C. Shan, L. Yang, H. Hu, Q. Wang, P. C. Lan, Y. Li, L. Wojtas, S. Ma and H. Xing, Efficient separation of xylene isomers by a guest-responsive metal-organic framework with rotational anionic sites, *Nat. Commun.*, 2020, **11**, 5456.

22 A. Cadiau, K. Adil, P. M. Bhatt, Y. Belmabkhout and M. Eddaoudi, A metal-organic framework-based splitter for separating propylene from propane, *Science*, 2016, **353**, 137–140.

23 L. F. Yang, X. L. Cui, Z. Q. Zhang, Q. W. Yang, Q. L. Ren and H. B. Xing, An Asymmetric Anion-Pillared Metal–Organic Framework as a Multisite Adsorbent Enables Simultaneous Removal of Propyne and Propadiene from Propylene, *Angew. Chem., Int. Ed.*, 2018, **57**, 13145–13149.

24 D. Sensharma, D. J. O'Hearn, A. Koochaki, A. A. Bezrukov, N. Kumar, B. H. Wilson, M. Vandichel and M. J. Zaworotko, The First Sulfate-Pillared Hybrid Ultramicroporous Material, SOFOUR-1-Zn, and Its Acetylene Capture Properties, *Angew. Chem., Int. Ed.*, 2022, **61**, e202116145.

25 H. S. Scott, N. Ogiwara, K.-J. Chen, D. G. Madden, T. Pham, K. Forrest, B. Space, S. Horike, J. J. Perry IV, S. Kitagawa and M. J. Zaworotko, Crystal engineering of a family of hybrid ultramicroporous materials based upon interpenetration and dichromate linkers, *Chem. Sci.*, 2016, **7**, 5470–5476.

26 Y. Zhang, L. Yang, L. Wang, S. Duttwyler and H. Xing, A Microporous Metal-Organic Framework Supramolecularly Assembled from a $Cu^{II}$ Dodecaborate Cluster Complex for Selective Gas Separation, *Angew. Chem., Int. Ed.*, 2019, **58**, 8145–8150.

27 Y. Zhang, L. Yang, L. Wang and H. Xing, Pillar iodination in functional boron cage hybrid supramolecular frameworks for high performance separation of light hydrocarbons, *J. Mater. Chem. A*, 2019, **7**, 27560–27566.

28 Y. Zhang, J. Hu, R. Krishna, L. Wang, L. Yang, X. Cui, S. Duttwyler and H. Xing, Rational Design of Microporous MOFs with Anionic Boron Cluster Functionality and Cooperative Dihydrogen Binding Sites for Highly Selective Capture of Acetylene, *Angew. Chem., Int. Ed.*, 2020, **59**, 17664–17669.

29 Y. Zhang, L. Wang, J. Hu, X. Cui and H. Xing, Solvent-dependent supramolecular self-assembly of boron cage pillared metal-organic frameworks for selective gas separation, *CrystEngComm*, 2020, **22**, 2649–2655.

30 L. Wang, W. Sun, Y. Zhang, N. Xu, R. Krishna, J. Hu, Y. Jiang, Y. He and H. Xing, Interpenetration Symmetry Control Within Ultramicroporous Robust Boron Cluster Hybrid MOFs for Benchmark Purification of Acetylene from Carbon Dioxide, *Angew. Chem., Int. Ed.*, 2021, **60**, 22865–22870.

31 W. Sun, J. Hu, S. Duttwyler, L. Wang, R. Krishna and Y. Zhang, Highly selective gas separation by two isostructural boron cluster pillared MOFs, *Sep. Purif. Technol.*, 2022, **283**, 120220.

32 L. Wang, T. Jiang, S. Duttwyler and Y. Zhang, Supramolecular Cu(II)-dipyridyl frameworks featuring weakly coordinating dodecaborate dianions for selective gas separation, *CrystEngComm*, 2021, **23**, 282–291.

33 (*a*) J. C. Axtell, L. M. A. Saleh, E. A. Qian, A. I. Wixtrom and A. M. Spokoyny, Synthesis and Applications of Perfunctionalized Boron Clusters, *Inorg. Chem.*, 2018, **57**, 2333–2350; (*b*) I. B. Sivaev, V. I. Bregadze and S. Sjöberg, Chemistry of closo-Dodecaborate Anion $[B_{12}H_{12}]^{2-}$: A Review, *Collect. Czech. Chem. Commun.*, 2002, **67**, 679–727; (*c*) K. I. Assaf, M. S. Ural, F. Pan, T. Georgiev, S. Simova, K. Rissanen, D. Gabel and W. M. Nau, Water Structure Recovery in Chaotropic Anion Recognition: High-Affinity Binding of Dodecaborate Clusters to γ-Cyclodextrin, *Angew. Chem., Int. Ed.*, 2015, **54**, 6852–6856; (*d*) X. Zhao, Z. Yang, H. Chen, Z. Wang, X. Zhou and H. Zhang, Progress in three-dimensional aromatic-like closo-dodecaborate, *Coord. Chem. Rev.*, 2021, **444**, 214042.

34 (*a*) Y. Zhang, Y. Sun, F. Lin, J. Liu and S. Duttwyler, Rhodium(III)-Catalyzed Alkenylation-Annulation of closo-Dodecaborate Anions through Double B-H Activation at Room Temperature, *Angew. Chem., Int. Ed.*, 2016, **55**, 15609–15614; (*b*) Y. Zhang, T. Wang, L. Wang, Y. Sun, F. Lin, J. Liu and S. Duttwyler, RhIII-Catalyzed Functionalization of closo-Dodecaborates by Selective B-H Activation: Bypassing Competitive C-H Activation, *Chem. – Eur. J.*, 2018, **24**, 15812–15817; (*c*) Y. Zhang, J. Liu and S. Duttwyler, $Rh^{III}$-Catalyzed Functionalization of *closo*-Dodecaborates by Selective B-H Activation: Bypassing Competitive C-H Activation, *Eur. J. Inorg. Chem.*, 2015, 5158–5162; (*d*) P.-F. Cui, X.-R. Liu, Y.-J. Lin, Z.-H. Li and G.-X. Jin, Highly Selective Separation of Benzene and Cyclohexane in a Spatially Confined Carborane Metallacage, *J. Am. Chem. Soc.*, 2022, **144**, 6558–6565.

35 S. Mukherjee, Y. He, D. Franz, S. Q. Wang, W. R. Xian, A. A. Bezrukov, B. Space, Z. Xu, J. He and M. J. Zaworotko, Halogen-$C_2H_2$ Binding in Ultramicroporous Metal-Organic Frameworks (MOFs) for Benchmark $C_2H_2/CO_2$ Separation Selectivity, *Chem. – Eur. J.*, 2020, **26**, 4923–4929.

36 H. Zeng, M. Xie, Y. L. Huang, Y. F. Zhao, X. J. Xie, J. P. Bai, M. Y. Wan, R. Krishna, W. G. Lu and D. Li, Induced Fit of $C_2H_2$ in a Flexible MOF Through Cooperative Action of Open Metal sites, *Angew. Chem., Int. Ed.*, 2019, **58**, 8515–8519.

37 S. Dutta, S. Mukherjee, O. T. Qazvini, A. K. Gupta, S. Sharma, D. Mahato, R. Babarao and S. K. Ghosh, Three-in-One $C_2H_2$-Selectivity-Guided Adsorptive Separation across an Isoreticular Family of Cationic Square-Lattice MOFs, *Angew. Chem., Int. Ed.*, 2022, **61**, e202114132.

38 L. Z. Liu, Z. Z. Yao, Y. X. Ye, L. J. Chen, Q. J. Lin, Y. S. Yang, Z. J. Zhang and S. C. Xiang, Robustness, Selective Gas Separation, and Nitrobenzene Sensing on Two Isomers of Cadmium Metal-Organic Frameworks Containing Various Metal-O-Metal Chains, *Inorg. Chem.*, 2018, **57**, 12961–12968.

39 H. Lv, Y. Li, Y. Xue, Y. Jiang, S. Li, M. Hu and Q. Zhai, Systematic Regulation of $C_2H_2/CO_2$ Separation by 3p-Block Open Metal Sites in a Robust Metal-Organic Framework Platform, *Inorg. Chem.*, 2020, **59**(7), 4825–4834.

40 J. Reynolds, K. Walsh, B. Li, P. Kunal, B. Chen and S. Humphrey, Highly selective room temperature acetylene sorption by an unusual triacetylenic phosphine MOF, *Chem. Commun.*, 2018, **54**, 9937–9940.

41 R. Liu, Q. Y. Liu, R. Krishna, W. J. Wang, C. T. He and Y. L. Wang, Water-Stable Europium 1,3,6,8-Tetrakis(4-carboxylphenyl)pyrene Framework for Efficient $C_2H_2/CO_2$ Separation, *Inorg. Chem.*, 2019, **58**, 5089–5095.

42 J. Pei, H.-M. Wen, X.-W. Gu, Q.-L. Qian, Y. Yang, Y. Cui, B. Li, B. Chen and G. Qian, Dense Packing of Acetylene in a Stable and Low-Cost Metal-Organic Framework for Efficient $C_2H_2/CO_2$ Separation, *Angew. Chem., Int. Ed.*, 2021, **60**, 25068–25075.

43 L. Zhang, K. Jiang, L. Yang, L. Li, E. Hu, L. Yang, K. Shao, H. Xing, Y. Cui, Y. Yang, B. Li, B. Chen and G. Qian, Benchmark $C_2H_2/CO_2$ Separation in an Ultra-Microporous Metal–Organic Framework via Copper(I)-Alkynyl Chemistry, *Angew. Chem., Int. Ed.*, 2021, **60**, 15995–16002.

44 J. Lee, C. Y. Chuah, J. Kim, Y. Kim, N. Ko, Y. Seo, K. Kim, T. H. Bae and E. Lee, Separation of Acetylene from Carbon Dioxide and Ethylene by a Water-Stable Microporous Metal–Organic Framework with Aligned Imidazolium Groups inside the Channels, *Angew. Chem., Int. Ed.*, 2018, **57**, 7869–7873.

45 Y. Peng, T. Pham, P. Li, T. Wang, Y. Chen, K. Chen, K. Forrest, B. Space, P. Cheng, M. Zaworotko and Z. Zhang, Robust Ultramicroporous Metal-Organic Frameworks with Benchmark Affinity for Acetylene, *Angew. Chem., Int. Ed.*, 2018, **57**, 10971–10975.

46 Y. Ye, Z. Ma, R. Lin, R. Krishna, W. Zhou, Q. Lin, Z. Zhang, S. Xiang and B. Chen, Pore Space Partition within a Metal–Organic Framework for Highly Efficient $C_2H_2/CO_2$ Separation, *J. Am. Chem. Soc.*, 2019, **141**, 4130–4136.

47 J. Zhang and X. Chen, Optimized Acetylene/Carbon Dioxide Sorption in a Dynamic Porous Crystal, *J. Am. Chem. Soc.*, 2009, **131**, 5516–5521.

48 S. Chen, N. Behera, C. Yang, Q. Dong, B. Zheng, Y. Li, Q. Tang, Z. Wang, Y. Wang and J. Duan, A chemically stable nanoporous coordination polymer with fixed and free $Cu^{2+}$ ions for boosted $C_2H_2/CO_2$ separation, *Nano Res.*, 2021, **14**, 546–553.

49 X. Duan, Q. Zhang, J. Cai, Y. Yang, Y. Cui, Y. He, C. Wu, R. Krishna, B. Chen and G. Qian, A new metal–organic framework with potential for adsorptive separation of methane from carbon dioxide, acetylene, ethylene, and ethane established by simulated breakthrough experiments, *J. Mater. Chem. A*, 2014, **2**, 2628–2633.

50 Y. Ye, S. Xian, H. Cui, K. Tan, L. Gong, B. Liang, T. Pjam, H. Pandey, R. Krishna, P. Lan, K. Forrest, B. Space, T. Thonhauser, J. Li and S. Ma, Metal–Organic Framework Based Hydrogen-Bonding Nanotrap for Efficient Acetylene Storage and Separation, *J. Am. Chem. Soc.*, 2022, **144**, 1681–1689.

51 Z. Niu, X. Cui, T. Pham, G. Verma, P. C. Lan, C. Shan, H. Xing, K. A. Forrest, S. Suepaul, B. Space, A. Nafady, A. M. Al-Enizi and S. Ma, A MOF-based Ultra-Strong Acetylene Nano-trap for Highly Efficient $C_2H_2/CO_2$ Separation, *Angew. Chem., Int. Ed.*, 2021, **60**, 5283–5288.

 

52 H. Li, C. Liu, C. Chen, Z. Di, D. Yuan, J. Pang, W. Wei, M. Wu and M. Hong, An Unprecedented Pillar-Cage Fluorinated Hybrid Porous Framework with Highly Efficient Acetylene Storage and Separation, *Angew. Chem., Int. Ed.*, 2021, **60**, 7547–7552.

53 P. Li, Y. He, Y. Zhao, L. Weng, H. Wang, R. Krishna, H. Wu, W. Zhou, M. O'Keeffe, Y. Han and B. Chen, A Rod-Packing Microporous Hydrogen-Bonded Organic Framework for Highly Selective Separation of $C_2H_2/CO_2$ at Room Temperature, *Angew. Chem., Int. Ed.*, 2015, **54**, 574–577.

54 (*a*) K. J. Chen, D. G. Madden, S. Mukherjee, T. Pham, K. A. Forrest, A. Kumar, B. Space, J. Kong, Q. Y. Zhang and M. J. Zaworotko, Synergistic sorbent separation for one-step ethylene purification from a four-component mixture, *Science*, 2019, **366**, 241–246; (*b*) X. Li, J. Wang, N. Bai, X. Zhang, X. Han, L. Silva, C. G. Morris, S. Xu, D. M. Wilary, Y. Sun, Y. Cheng, C. A. Murray, C. C. Tang, M. D. Frogley, G. Cinque, T. Lowe, H. Zhang, A. J. Ramirea-Cuesta, K. M. Thomas, L. W. Bolton, S. Yang and M. Schroder, Refinement of pore size at sub-angstrom precision in robust metal-organic frameworks for separation of xylenes, *Nat. Commun.*, 2020, **11**, 4280; (*c*) J. W. Cao, S. Mukherjee, T. Pham, Y. Wang, T. Wang, T. Zhang, X. Jiang, H. J. Tang, K. A. Forrest, B. Space, M. J. Zaworotko and K. J. Chen, One-step ethylene production from a four component gas mixture by a single physisorbent, *Nat. Commun.*, 2021, **12**, 6507.